Energy Reports 7 (2021) 9035–9045

Contents lists available at ScienceDirect

Energy Reports

journal homepage: www.elsevier.com/locate/egyr

Research paper

Parameters identification and optimization of photovoltaic panels under real conditions using Lambert W-function

Dris Ben hmamou [b], Mustapha Elyaqouti [c], Elhanafi Arjdal [b], Ahmed Ibrahim [a,e,h,*], H.I. Abdul-Ghaffar [d,g], Raef Aboelsaud [a,e,h], Sergey Obukhov [e], Ahmed A. Zaki Diab [f]

[a] Electrical Power & Machines Department, Faculty of Engineering, Zagazig University, Egypt
[b] Laboratory of Electronics, Signal Processing and Physical Modeling, Faculty of Sciences of Agadir Ibn Zohr University, BP 8106, 80000 Agadir, Morocco
[c] Materials and Renewable Energy Laboratory, Agadir Faculty of Sciences, Ibn Zohr University, BP 8106, 80000 Agadir, Morocco
[d] Mechatronics Department, Egyptian-Korean Faculty for Industry and Energy Technology, Bani Swief Technological University, Bani Swief, Egypt
[e] National Research Tomsk Polytechnic University, Tomsk 634050, Russia
[f] Electrical Engineering Department, Faculty of Engineering, Minia University, Minia 61111, Egypt
[g] New Urban Communities Authority, New Minia City, Minia, Egypt
[h] Institute of Applied Mathematics and Computer Science, Tomsk State University, Tomsk, Russsia

ARTICLE INFO

Article history:
Received 14 July 2021
Received in revised form 9 November 2021
Accepted 11 November 2021
Available online 6 December 2021

Keywords:
Photovoltaic
Single diode model
Shell SP70 monocrystalline silicon
Shell ST40 thin film
KC200GT Polycrystalline Silicon
Lambert W-function

ABSTRACT

This paper proposes a new approach based on Lambert W-function to extract the electrical parameters of photovoltaic (PV) panels. This approach can extract the optimal electrical characteristics of the PV panel under variable conditions of irradiation and temperature. Three benchmarking panels (shell SP70 monocrystalline silicon, shell ST40 thin film, and KC200GT Polycrystalline Silicon) are demonstrated and analyzed considering the electrical characteristics provided by the manufacturers. A comprehensive assessment is carried out under different weather condition to validate the capability and the robustness of the proposed approach. Furthermore, the simulated output characteristics of the three modules Photovoltaic are almost comparable and reproduce faithfully the manufacturer's experimental data The novelty of this study is the using a new hybrid analytical and numerical method that straight forward and effective given value of Root mean square error less than those obtained by others methods that indicate the estimated results are very close to the experimental values provided by the manufacturers.

1. Introduction

In the production of renewable energy like solar, photovoltaic and wind energy which are clean and the technology related to these green energies, has an important goal in filling the country's electricity shortage. During the last decades, several studies have been carried out by several researchers for modeling photovoltaic systems and their technology by using various procedures and evaluating the number of parameters using varieties simulation software. The current produced with solar cells is directly dependent on the types and the sunlight reaching of solar cells. Fig. 1 shows the operating principle of the solar cell.

However, there are several types of solar cells, such as more than 90% of the solar cells currently made worldwide consist of wafer-based silicon cells (Louwen and Van Sark, 2019). They are called mono-crystalline or multi-crystalline silicon solar cells. Wafer-based silicon solar cells are approximately 200 μm thick. Another important family of solar cells can be manufactured at lower cost in large production quantities is based on thin-films, which are approximately from 1 to 2 μm thick and therefore require significantly less active semiconducting material. However, they indicate lower efficiencies than wafer-based silicon solar cells, which mean that more exposure surface and material for the installation is required for a similar performance. The photovoltaic module are constructed with a number of solar cells electrically connected in series or parallel electrical arrangements to each other and mounted in a single support structure or frame to produce any required voltage and current combination. There are two main types of photovoltaic system. Grid connected systems are connected to the grid and inject the electricity into the grid (Elsadd et al., 2021). For protect distribution and transmission systems of the power generation networks, the directional over current relays are widely preferred (Akdag and Yeroglu,

* Correspondence to: Electrical Engineering Department, Faculty of Engineering, Minia University, Minia 61111, Egypt.
E-mail addresses: ibragim@tpu.ru (A. Ibrahim), a.diab@mu.edu.eg (A.A.Z. Diab).

https://doi.org/10.1016/j.egyr.2021.11.219

Nomenclature

STCs	Standard Test Conditions
G	Solar irradiance (W/m^2)
G_n	Solar irradiance at STCs (1000 W/m^2)
T	PV cell temperature (°C)
T_n	PV cell temperature at STCs (°C)
q	Electric charge of an electron ($1.602.10^{-19}$ C)
K	Boltzmann constant ($1.381.10^{-23}$ J/K)
n	diode ideality factor
K_v	Open circuit voltage temperature coefficient (V/°C)
I_{ph}	Photocurrent (A)
RMSE	Root Mean Square Error (A)
$P_{\max\_esti}$	Estimated power at the maximum power point (W)
$P_{\max\_exp}$	Experimental power at the maximum power point (W)
N_s	Number of cells connected in series
ARE	Average Relative Error
IAE	Individual Absolute Error
MPP	Maximum power point
R_S	Series resistance (Ω)
R_{sn}	Series resistance at STCs (Ω)
R_{sh}	Shunt resistance (Ω)
R_{shn}	Shunt resistance at STCs (Ω)
I_{on}	Reverse saturation current of the diode at STCs (A)
I_o	Reverse saturation current of the diode (A)
V_{oc}	Open circuit voltage of the PV panel (V)
V_{ocn}	Open circuit voltage of the PV panel at STCs (V)
K_i	Short circuit current temperature coefficient (A/°C)
I_{phn}	Photocurrent at STCs (A)
I_{sc}	Short circuit current of the PV module (A)
CIS	Copper Indium Diselenide
I_{scn}	Short circuit current of the PV module at STCs (A)
E_{gn}	Gap energy of solar cell at STCs (eV)
E_g	Gap energy of solar cell (eV)
I–V	Current–Voltage characteristic

2021). Krakowski et al. (2021) present and compared two different proprietary real-time simulation systems. The first one is based on DAQ-cards and second one is based on pure IEC 61850 services utilized for power system protections testing. Kong and Meliopoulos (2021) Study on effects of DSE-Based instrumentation channel error correction on protective relays (Kong and Meliopoulos, 2021). For this reason, the direct current produced by the solar modules is converted into a grid-compatible alternating current. However, solar power plants can also be operated without the grid and are then called autonomous systems or off-grid systems. In this study we search to build an accurate photovoltaic circuit model with any circuit simulator using Matlab program, but the manufacturers only provide a few electrical and thermal characteristic which are obtained at STCs of irradiation and temperature. So to find a solution to this problem the

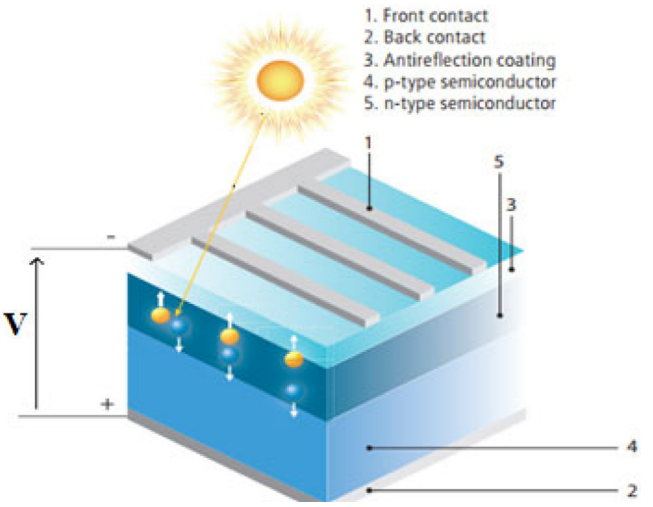

Fig. 1. The operating principle of a photovoltaic cells (Louwen and Van Sark, 2019).

modeling method should be investigated that would find all of this parameters in order to obtain the desired photovoltaic model. Regarding this issue Different techniques have been developed in the literature.

The PV parameters can be extracted by three common approaches:

(a) Analytical approach based on the derivation of mathematical equations and provides simple identification of all PV parameters at small time of computation. The accuracy of this approach is depends the main points of I–V characteristic curves were utilized such us I_{sc}, V_{oc} and the Maximum power point (MPP). The downside of this approach does not reflect the real operating conditions and has less accurate than well-known approaches (Ma et al., 2013a,b; Hejri et al., 2014). Toledo and Blanes (2016) used Analytical and Quasi-Explicit (AQE) method to coordinates of four arbitrary points of the I–V characteristic and their slopes. Ruschel et al. (2016) study the shunt resistance dependence on the irradiance level in order to evaluate some of the usual expressions proposed on the literature. Lo et al. (2012) employed an analytical method able to evaluate the operating current with a high degree of accuracy, even during days perturbed by very variable conditions of solar irradiance. Tong and Pora (2016) adopted an approach by using the scanning strategy for finding the parameters that minimize the cost function. Dongue et al. (2013) use the analytical approach to replicate the electrical behaviors of operating PV modules based on some simplified assumptions. Batzelis and Papathanassiou (2015) used Lambert W based analytical method very useful for various operating conditions of PV modules.

(b) The numerical extraction method usually use non-linear optimization techniques, such as: Newton–Raphson methods (NRM) (Villalva et al., 2009a,b), conductivity method (CM) (Chegaar et al., 2013) or the Levenberg–Marquardt (LM) algorithm (Hejri et al., 2014) to identify the parameters of the simulation models of the PV system. For being applicable and solving the equation for the extraction of the PV cells parameters, the fitness function need to be continuous, convex and differentiable. But, the large number of unknown parameters complicates the extraction's procedure.

(c) The last one is meta-heuristic approaches characterized by their global search point and their soft computing algorithms. These approaches are attractive due to their global search capability to deal with the nonlinear problems without the need for the complex calculation of the objective function and initialization constraints (Zagrouba et al., 2010; Khan et al., 2010; El-Naggar et al., 2012). Among these methods, we can find: Balzani et al. (0000) modeled the behavior of PV module using ANN method based on the Levenberg–Marquardt function. Elhagry et al. (1997) adopted a Fuzzy Regression model to predict the parameters of single-diode model based on limited amount of measured data. Bendib et al. (2016) are used Fuzzy Logic (FL) method for organic cells to fit the calculated I–V curve to the experimental data. Jervase et al. (2011) employed Genetic Algorithm (GA) to extract the parameters of two diode model and (Zagrouba et al., 2010) for the single diode R_P-model. The both authors used the measured I–V curves of several PV cells and modules. Also, Ismail et al. (2013) applies GA to find the global optimal parameters values of a PV module that used to predict the output current and voltage of the PV modules at real operating conditions. The performance of the GA was shown to surpass that of the conventional quasi-Newton method. Ye et al. (2009), Macabebe et al. (2011) and Qin and Kimball (2011) applied Particle Swarm Optimization (PSO) to extract all parameters of the single and two-diode models from the I–V curves for several types of cells and modules. This approach requires computing both the velocity and position equations for each solution. Wei et al. (2011) adopted the chaos particle swarm optimization algorithm (CPSO) to extract the parameters of the single diode R_P-model by utilizing to reinitiate the stagnant particles. Using the digitized datasheet I–V characteristic, Teixeira et al. (2010) employed Differential Evolution (DE) to extract the modules parameters at different values of G and T. Ishaque and Salam (2011) adopted DE for evaluated the speed and accuracy of extracting parameters of the two-diode model using two variation of DE. The Boundary based denoted B-DE and the Penalty based denoted P-DE. This last type is also used with Ishaque et al. (2012). In Ishaque et al. (2011), the authors are using an hybrid approach analytical and DE with only information available on the manufacturer's datasheet. I_{PV} and I_0 were determined analytically, while n, R_s, and R_{sh} were obtained by optimizing the slope equation at MPP. El-Naggar et al. (2012) employed Simulated Annealing (SA) to identify the parameters of the single and two-diode models for different cells and module, they have shown that SA has better accuracy compared to well-known conventional optimization approach. In Alhajri et al. (2012), all parameters of single and double diode are estimated by applying the Pattern Search (PS) approach that was found to yield better accuracy compared to conventional optimization techniques. Rajasekar et al. (2013) applied a hybrid method analytical and Bacteria Foraging algorithm modeling (BFA) to compute all parameters of the single diode R_P-model. In Ma et al. (2013a,b) the authors employed Cuckoo Search (CS) to extract the parameters of the conventional single diode model for several cells and modules. Askarzadeh and Rezazadeh (2012) applied two variants of Harmony Search (HS) method. The first one is grouping-based global harmony search denoted GGHS, and the second is innovative global harmony search denoted IGHS to identify the parameters of the single diode and the double-diode model for PV cells. The same authors in Askarzadeh and Rezazadeh (2013a,b) are also employed Artificial Bee Swarm Optimization (ABSO) and Bird Mating Optimizer (BMO) to extract the parameters of the single and two-diode models for PV cells and modules to calculate the MPPT of the corresponding I–V curve. Also, Askarzadeh and Coelho (2015) developed a simplified method of BMO denoted simplified BMO (SBMO) to estimate the parameters of the single diode R_P-model for an amorphous silicon PV module.

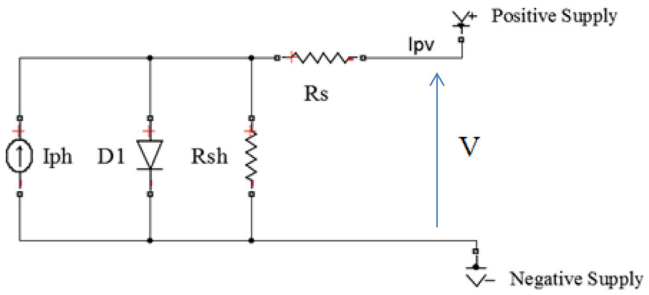

Fig. 2. The equivalent circuit of the photovoltaic module.

In this study, the single diode model are adopted for modeling the photovoltaic module using an analytical method based on the Lambert W-function adopted by the different authors (Nassar-Eddine et al., 2016; Chen et al., 2018; García-Sánchez et al., 2017; Ghani et al., 2014).

The remainder of this paper is organized in the following manner. After an introduction, Section 2 describes the electrical parameters and the modeling of the specific photovoltaic panels used in this study. In Section 3, we present the electrical characterization of the photovoltaic panels using the Lambert W-function. Finally, we present in Section 4, all obtained results regarding the electrical modeling and characterization of used PV modules.

2. Parameters and model of the specific photovoltaic panels

2.1. Identification of the photovoltaic module

In this study and in order to obtain a better validation of our approach, we used three different technologies of photovoltaic modules such as monocrystalline shell SP70 (Shell SP70, 2021), polycrystalline Kyocera KC200GT (Kyocera KC200GT, 2021) and the thin film Shell ST40 based on Copper Indium Diselenide (CIS) (Shell ST40, 2021). The various parameters of these panels are summarized in Table 1.

2.2. Modeling of the photovoltaic module

The photovoltaic module is formed with N_s photovoltaic cells connected in series. It can be represented by the single diode model shown in Fig. 2:

The mathematical equation describes the output characteristic I–V of the PV module and the performance of the PV module is given by Eq. (1):

$$I_{pv} = I_{ph} - I_o \times \left\{ \exp\left[\frac{q(V + R_S \times I_{pv})}{n \times K.T.Ns} \right] - 1 \right\} - \frac{V + R_S \times I_{pv}}{Rsh} \quad (1)$$

where: I_{pv} and V are the output current and output voltage of PV module respectively, I_{ph} is the photocurrent generated bay photovoltaic module under illumination, I_o is the reverse saturation current of the diode, n is the diode ideality factor depends on PV technology and have been assumed ranging from 1 to 2, R_S is the series resistance used to characterize the resistance of

Table 1
Electrical characteristic data at STCs of three kinds of photovoltaic modules.

Electrical characteristic	Kyocera KC200GT	Shell SP70	Shell ST40
Open circuit voltage V_{oc} (V)	32.9	21.4	23.3
Short circuit current I_{sc} (A)	8.21	4.7	2.68
Output Voltage at MPP, V_{mp} (V)	26.3	16.5	16.6
Output Current at MPP, I_{mp} (A)	7.61	4.25	2.41
Short circuit current temperature coefficient, k_i (A/°C)	0.0032	0.002	0.00035
Open circuit voltage temperature coefficient, k_v (V/°C)	−0.123	−0.076	−0.1
Maximum power at STCs P_{max}	200	70	40
Number of cells connected in series, N_s	54	36	36

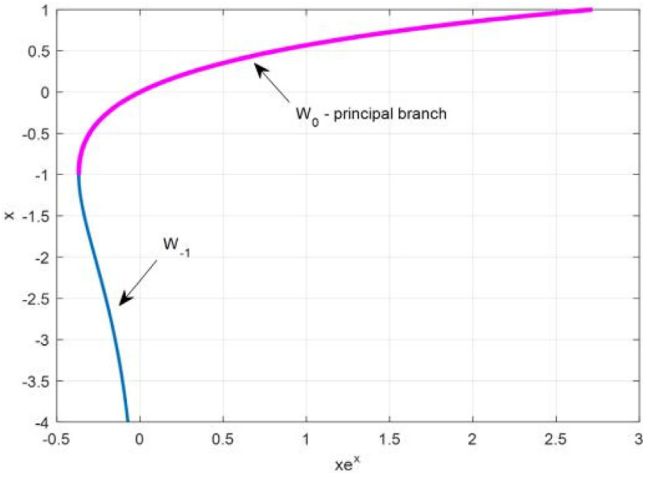

Fig. 3. Graphic representation of the Lambert W-function (Ćalasan et al., 2020).

electrode surface, R_{sh} is the shunt resistance used to characterize the leakage current of P-N junction, K is the Boltzmann constant ($1.38.10^{-23}$ J/K), q is the electron charge ($1.67.10^{-19}$ C), N_s is the number of cells connected in series and finally T is the cell temperature.

3. Characterization of the photovoltaic panel using the Lambert W-function

From Eq. (1), we notice that it has a high degree of non-linearity. This equation can be solved using iterative Newton–Raphson method (Villalva et al., 2009a,b; Stornelli et al., 2019; Agwa et al., 2020) or by using Lambert W-function (Peng et al., 2013, 2018; Ćalasan et al., 2020; Cubas et al., 2014; Javier Toledo et al., 2018; Toledo and Blanes, 2016). This last function is presented in Fig. 3.

In this study, we employed the inverse branch of the Lambert W-function that whose expression is given by $Z = X.e^X$ in order to find the exact solution of Eq. (1). The strategy adopted is to convert the expression of the output current into one of the form $Z = X.e^X$ and then to find the expression of X using the W-function. From Eq. (1) and after rearrangement, we can obtain the following expression:

$$\left[\frac{q\,(I_o.R_s.R_{sh})}{n.K.T.\,(R_s+R_{sh})}.\exp\left(\frac{.q.\,(V+I_{pv}.R_s)}{n.K.T}\right)\right] \cdot \exp\left[\frac{q\,(I_o.R_s.R_{sh})}{n.K.T.\,(R_s+R_{sh})}.\exp\left(\frac{.q.\,(V+I_{pv}.R_s)}{n.K.T}\right)\right] = \frac{q(I_o.R_s.R_{sh})}{n.K.T.(R_s+R_{sh})}.\exp\left(\frac{R_s.q.\,(I_{ph}.R_{sh}+I_o.R_s+V)}{n.K.T.\,(R_s+R_{sh})}\right) \quad (2)$$

Based on the following changes in variables:

$$X = \left[\frac{q\,(I_o.R_s.R_{sh})}{n.K.T.\,(R_s+R_{sh})}.\exp\left(\frac{.q.\,(V+I_{pv}.R_s)}{n.K.T}\right)\right] \quad (3)$$

$$Z = \frac{q\,(I_o.R_s.R_{sh})}{n.K.T.\,(R_s+R_{sh})}.\exp\left(\frac{R_s.q.\,(I_{ph}.R_{sh}+I_o.R_s+V)}{n.K.T.\,(R_s+R_{sh})}\right) \quad (4)$$

Then the Eq. (2) becomes:

$$X.e^X = Z \Leftrightarrow X = \text{lambertW}\,(Z) \quad (5)$$

Finally, the expression of output current of the photovoltaic module is indicated on the following expression:

$$I_{pv} = \frac{n.K.T}{q.R_s}\text{LambertW}\,(Z) - \frac{V-(I_{ph}+I_o).R_{sh}}{(R_{sh}+R_s)} \quad (6)$$

All this model's parameters are evaluated in a particular points of I–V characteristics curve such us the open circuit condition ($I = 0; V = V_{ocn}$) and the short circuit condition ($V = 0; I_{pv} = I_{scn}$). Then it possible to establish the following relations at STCs:
At short circuit condition:

$$I_{scn} = I_{phn} - I_{on}\times\left(e^{\frac{q\times(R_{sn}\times I_{scn})}{n\times K\times T\times N_s}} - 1\right) - \frac{R_{sn}\times I_{scn}}{R_{shn}} \quad (7)$$

At open circuit condition:

$$I_{phn} - I_{on}\times\left(e^{\frac{q\times(V_{ocn})}{n\times K\times T_n\times N_s}} - 1\right) - \frac{V_{ocn}}{R_{shn}} = 0 \quad (8)$$

$$I_{phn} = I_{on}\times\left(e^{\frac{q\times(V_{ocn})}{n\times K\times T_n\times N_s}} - 1\right) + \frac{V_{ocn}}{R_{shn}} \quad (9)$$

Taking into account the Eqs. (7) and (9), we will find:

$$I_{on} = (I_{scn} - \frac{V_{ocn} - R_{sn}\times I_{scn}}{R_{shn}}) \times e^{-\frac{q\times(V_{ocn})}{n\times K\times T_n\times N_s}} \quad (10)$$

Under standard test conditions (STCs), the derivative of the current I_{pv} with respect to the voltage V at ($I_{pv} = 0; V = V_{ocn}$) and at ($V = 0; I = I_{scn}$) gives respectively the two equations (11) and (12) (Abbassi et al., 2018). The mathematical meaning of these equations is shown in Fig. 4.

$$\left.\frac{dI_{pv}}{dV}\right|_{(I_{pv}=0;V=V_{ocn})} = -\frac{1}{R_{sn}} \quad (11)$$

$$\left.\frac{dI_{pv}}{dV}\right|_{(V=0;I_{pv}=I_{scn})} = -\frac{1}{R_{shn}} \quad (12)$$

As long as the manufacturers of photovoltaic modules almost gives the all experimental characteristics and electrical specifications under Standard Test Conditions (STCs), but the real conditions can be varied further. The parameters of the photovoltaic module are sensitive to the weather conditions changes, then all model parameters are obtained using the expressions as follows (Abbassi et al., 2018):

The saturation current of the diode is given by (13):

$$I_o = I_{on}.\left(\frac{T}{T_n}\right)^3.e^{\left[\frac{q.Eg.N_s}{n.K.T(1-\frac{T_n}{T})}\right]} \quad (13)$$

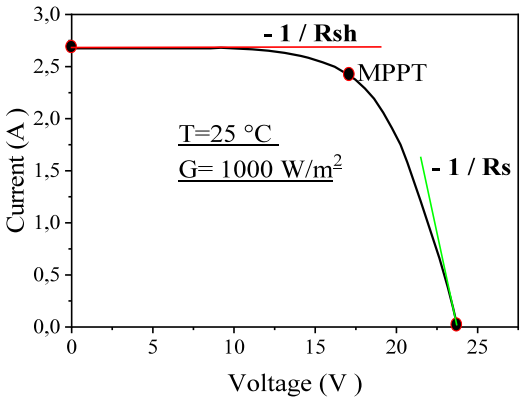

Fig. 4. Assumption at remarkable points.

The photo-current is given by (14):

$$I_{ph} = I_{phn} + K_i.(T - T_n).\left(\frac{G}{G_n}\right) \tag{14}$$

The open circuit voltage is given by (15):

$$V_{oc} = V_{ocn} - K_v.(T_n - T) + \frac{n.K.T.N_s}{q}.\ln\left(\frac{G}{G_n}\right) \tag{15}$$

The short circuit current is given by (16):

$$I_{sc} = (I_{scn} + K_i.(T - T_n)).\left(\frac{G}{G_n}\right) \tag{16}$$

The series and shunt resistances are expressed by (17) and (18) respectively:

$$R_s = R_{sn} - \left[\left(\frac{n.K.T}{q.I_0}\right).e^{\left(-\frac{q.Voc}{n.K.T}\right)}\right] \tag{17}$$

$$R_{sh} = R_{shn}.\left(\frac{G_n}{G}\right) \tag{18}$$

The gap energy E_g is depends of temperature which can be corrected based on Eq. (19) (Agwa et al., 2020).

$$E_g = E_{gn}\,[1 - 2.6677 \times (T - T_n)] \tag{19}$$

Where E_{gn} is the value of gap energy for the PV cells at STCs, $E_{gn} = 1.12$ eV for monocrystalline cells, $E_{gn} = 1.14$ eV for polycrystalline cells and $E_{gn} = 1$ eV for thin film based on Copper Indium Diselenide (CIS) (De Soto et al., 2006).

Finally the estimated power through the proposed method is obtained using the expression as follow:

$$P_{esti} = I_{pv} \times V \tag{20}$$

The goal is to find the value of ideality factor that makes the peak of the estimated P–V characteristic coincide with the experimental peak power at the (V_{mp}, I_{mp}) point. This requires several iterations until:

$$P_{max\_esti} \approx P_{max\_exp} \tag{21}$$

Where:

$$P_{max\_exp} = I_{mp} \times V_{mp} \tag{22}$$

Fig. 5 show the flowchart of extraction of all parameters using the proposed approach.

4. Results and discussion

4.1. Electricals characterization of the PV modules

The aim of this study is the extraction of PV module parameters using the hybrid approach that simulated in Matlab software.

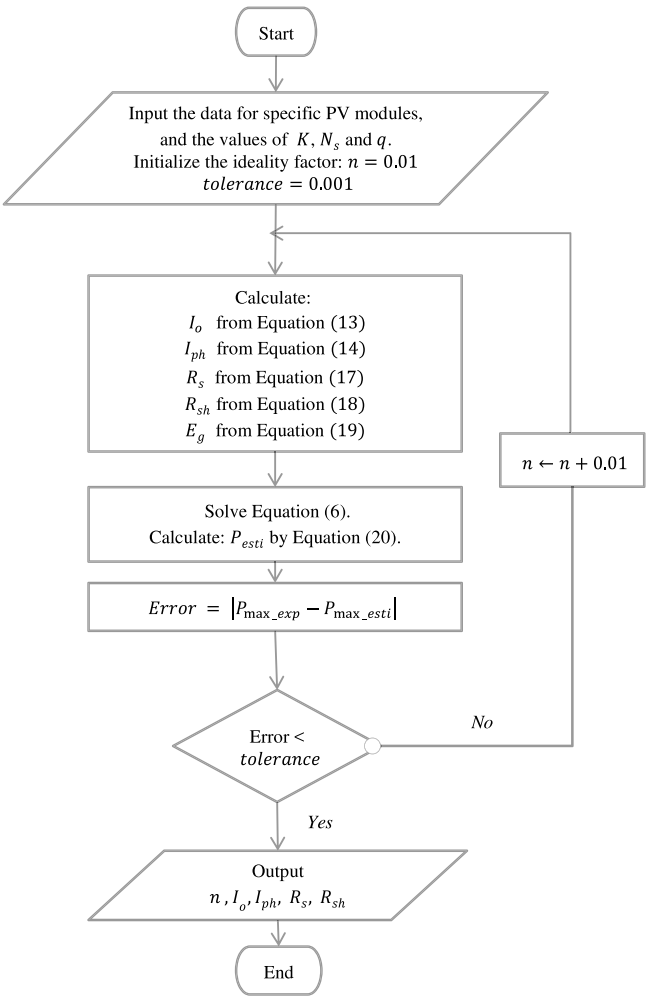

Fig. 5. Flowchart of extraction of all parameters model.

The remaining parameters are obtained once the estimated and experimental powers are equal. The five model parameters for the PV modules obtained from the proposed approach at STCs as illustrated in Table 2. The reliability of the proposed model is further justified by the comparing the obtained results with Wang's method (Wang et al., 2017) and Villalva's method (Villalva et al., 2009a,b).

The shunt resistance R_{sh} affect slope of the characteristic I–V between I_{sc} and MPP points, generally, it has a high value in order to KΩ. As shown in Table 2, R_{sh} obtained for Shell ST40 module using this method is higher than Wang's and Villalva's methods, and then we can verify better accuracy in the quasi constant current region. The Value of the series resistance R_S is very low and usually neglected (Tan et al., 2010; Benavides et al., 2008). This parameter affect slope of the curve in regions between MPP and V_{oc}. The values founded using the proposed method located between smaller than 1.4 Ω and larger than 0.35 Ω lead to better accuracy of the Wang's methods and Villalva's methods. The value of n, I_o and I_{pv} are almost similarly to the values obtained using Wang's and Villalva's methods.

4.2. Case of variable irradiation at fixed temperature

Using the parameters calculated by the proposed method, listed in Table 2, we can calculated and drawn the I–V characteristic for the PV modules studied by replacing the obtained

Table 2
Calculated model parameters of the proposed approach compared with Villalva's method (Villalva et al., 2009a,b) and Gang Wang's method (Wang et al., 2017).

PV modules	Method	n	I_{pv}(A)	I_o (A)	R_s (Ω)	R_{sh} (Ω)
Polycrystalline KC200GT	Proposed approach	0.984	8.2303	$1{,}960.10^{-10}$	0.3510	500
	Villalva's method	1.3	8.2136	$9{,}83.10^{-8}$	0.2260	508.99
	Gang Wang's method	1.3	8.2132	$9{,}83.10^{-8}$	0.2291	593.24
Monocrystalline Shell SP70	Proposed approach	0.9807	4.7215	$3{,}42.10^{-10}$	0.3860	163.10
	Villalva's method	1.3	4.7132	$8{,}76.10^{-8}$	0.4010	135.42
	Gang Wang's method	1.3	4.7132	$8{,}76.10^{-8}$	0.4081	145.44
Thin film Shell ST40	Proposed approach	1.1	2.6846	$3{,}42.10^{-10}$	1.4000	7520
	Villalva's method	1.6	2.6825	$3{,}89.10^{-7}$	1.3450	1465.8
	Gang Wang's method	1.6	2.6805	$3{,}89.10^{-7}$	1.3656	7301.6

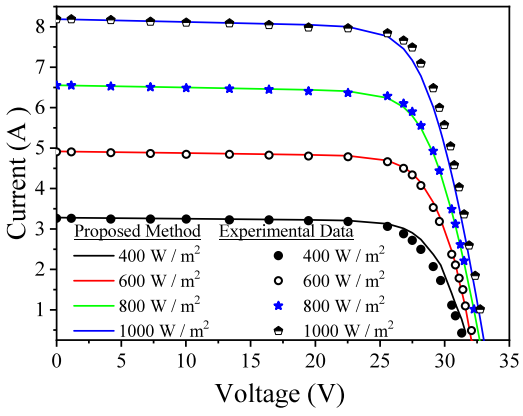

Fig. 6. The influence of the irradiation on the I–V characteristic for Kyocera KC200GT and comparison with experimental data.

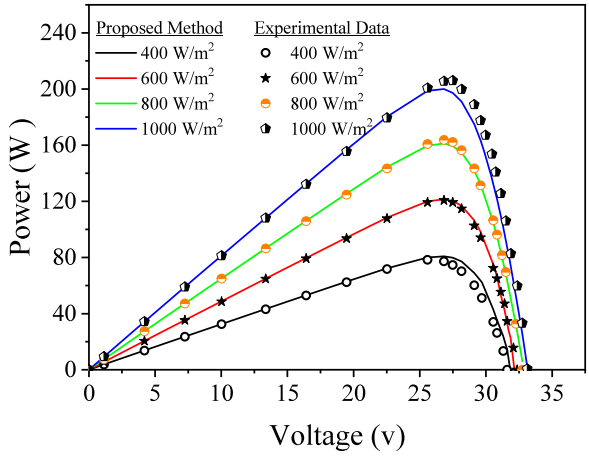

Fig. 7. The influence of the irradiation on the P–V characteristic for Kyocera KC200GT and comparison with experimental data.

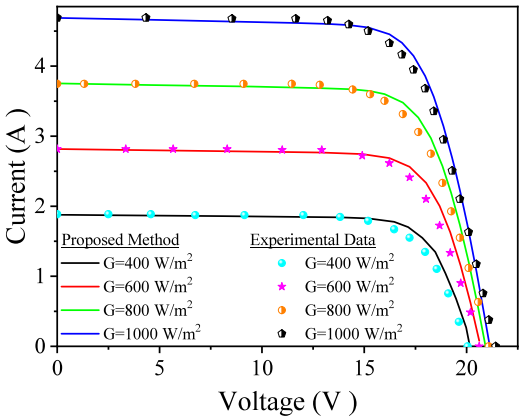

Fig. 8. The influence of the irradiation on the I–V characteristic for Shell SP70 and comparison with experimental data.

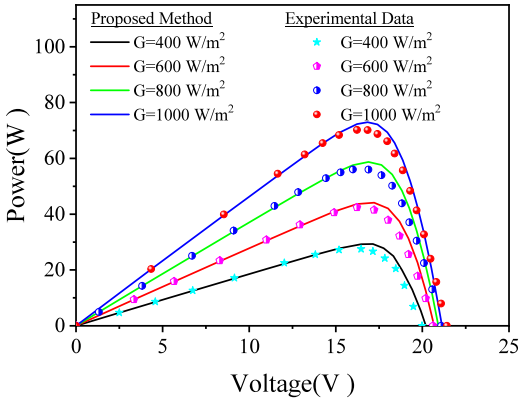

Fig. 9. The influence of the irradiation on the P–V characteristic for Shell SP70 and comparison with experimental data.

parameters in the Eq. (6) and incrementing the voltage from zero to the value V_{oc}. Validity of the obtained values from experimental data extracted from the manufacturer's datasheet of (Shell ST40.2021), (Kyocera KC200GT.2021) and (Shell SP70.2021) modules. First step in this study, we need to change the irradiation conditions from 400 to 1000 W/m^2 and the temperature maintained constant at 25° C. The response of the photovoltaic modules due to this effect is shown on Figs. 6 and 7 for Kyocera KC200GT module, Figs. 8 and 9 for Shell SP70 module and Figs. 10 and 11 for Shell ST40 module.

The obtained results indicate that the open circuit voltage increases slightly, but the short circuit current increases as the solar irradiance increases. It can be seen also, that the presents figures shown an excellent corresponding between theoretical and experimental curves, but we can notice a low accuracy and remarkable deviation at the vicinity of the maximum power point for KC200GT module at G = 1000 W/m^2, for Shell ST40 at G = 1000 W/m^2 and G = 800 W/m^2.

4.3. Case of variable temperature at fixed irradiation

In the second step we need to change the temperature conditions from 20 to 60 °C and the irradiation maintained constant at G=1000 W/m^2. Figs. 12 and 13 shows the computed curves at 1000 W/m^2 while the temperature change for Shell ST40 module and the reaction due to this effect: ————

The results show that when the temperature increases, the open circuit voltage decrease, while the short circuit current

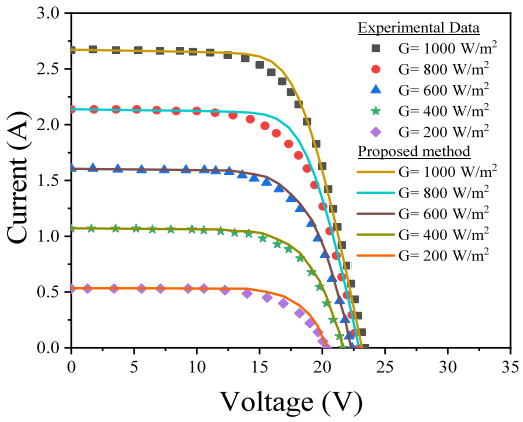

Fig. 10. The influence of the irradiation on the I–V characteristic for Shell ST40 and comparison with experimental data.

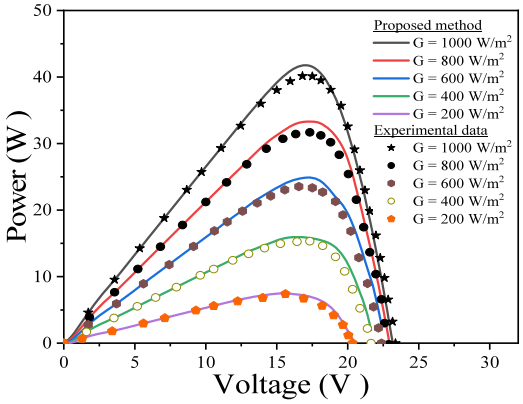

Fig. 11. The influence of irradiation on the P–V characteristic for Shell ST40 and comparison with experimental data.

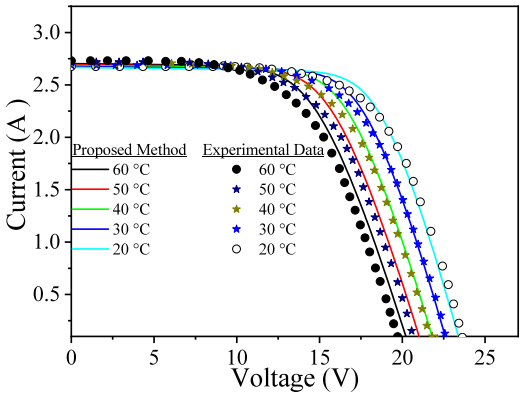

Fig. 12. The influence of the temperature on the I–V characteristic for Shell ST40 and comparison with experimental data.

remains constant which at high temperature. It presents the deviation between theoretical and experimental curves. The increase of short circuit current is justified by the fact that when the temperature increases, the thermal agitation also increasing which makes the interatomic spacing larger and the distance between the valence band of electrons and the conduction band decrease, thus more photons can easily reach the valence band and eventually create electron–hole pairs (Chennoufi et al., 2021).

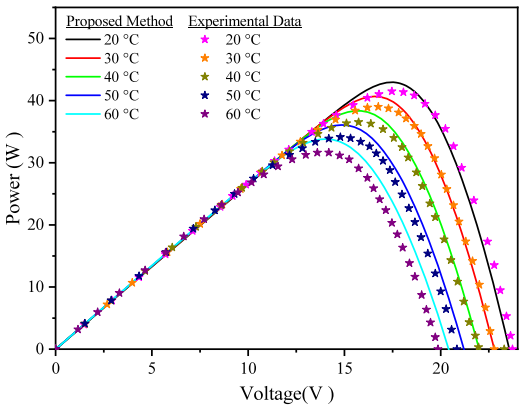

Fig. 13. The influence of the temperature on the P–V characteristic for Shell ST40 and comparison with experimental data.

4.4. More accuracy of the proposed method

The evaluation of the precision of the method considered is performed by calculating the Root Mean Square Error (RMSE), the Individual Absolute Error of output current (IAE) (Shinong et al., 2020; De Soto et al., 2006; Bellia et al., 2014) and the Average Relative Error (ARE) (Shinong et al., 2020). For *N* estimated or experimental values of output current, they are given by the expression shown at Eq. (23), (24) and (25) as follows:

$$\mathrm{RMSE} = \sqrt{\frac{\sum_{i=1}^{N}\left(I_{i,\mathrm{experimental}} - I_{i,\mathrm{estimated}}\right)^2}{N}} \tag{23}$$

$$\mathrm{IAE} = \left|I_{i,\mathrm{experimental}} - I_{i,\mathrm{estimated}}\right| \tag{24}$$

$$\mathrm{ARE} = \frac{1}{N}\sum_{i=1}^{N}\frac{\left|I_{i,\mathrm{estimated}} - I_{i,\mathrm{experimental}}\right|}{I_{i,\mathrm{experimental}}} \tag{25}$$

Where $I_{i,\mathrm{estimated}}$, $I_{i,\mathrm{experimental}}$, N are the estimated current, experimental current, number of estimated or experimental values of output current, respectively.

The Table 3 Presents the comparison between the Average Relative Errors (ARE) of the output current for Kyocera KC200GT, Shell SP70 and Shell ST40 module using the proposed method and those obtained by Shinong's approach (Shinong et al., 2020). It can be seen that all the computed ARE using a proposed method are better than those obtained by Shinong et al. It is indicating that the method adopted in this study is very effective and straight forward and given a good correlation between the estimated results and the results provided by the manufacturers. Fig. 14 shows the comparisons with the all values of ARE for Shell SP70 module obtained using the proposed method and Shinong's method.

The Root Means Square Error (RMSE) for Shell ST40 module are also calculated and summarized in Table 4 at different irradiation level compared with previously results obtained by other authors (Yahya-Khotbehsara and Shahhoseini, 2018; Ishaque et al., 2011; Babu and Gurjar, 2014; Wang et al., 2017).

The Root Mean Square Error (RMSE) of output current for Shell ST40 module when the temperature change is presented in Table 5. The Results shows that between the values T = 20 °C and T = 40 °C the proposed model has the least RMSE value compared to other methods.

Fig. 14 shows the comparison of the RMSE calculated using the proposed approach for Shell ST40 module with the other methods. We can see that between 200 W/m^2 and 800 W/m^{2}the Root mean square error of the proposed method is much smaller

Table 3
Comparison of average relative errors (ARE) of KC200GT, Shell SP70 and Shell ST40 module at real Environment conditions.

Solar cells	Environment conditions	ARE (%)	
		Proposed method	Shinong et al. (2020)
Kyocera KC200GT T = 25 °C	G = 400 W/m^2	4.35	5.49
	G = 600 W/m^2	1.26	8.46
	G = 800 W/m^2	1.68	6.90
	G = 1000 W/m^2	3.15	5.33
Shell SP70 T = 25 °C	G = 400 W/m^2	3.02	5.64
	G = 600 W/m^2	2.82	7.01
	G = 800 W/m^2	1.50	3.29
	G = 1000 W/m^2	2.58	4.31
Shell ST40 G = 1000 W/m^2	T = 20 °C	2.90	4.05
	T = 30 °C	3.05	3.74
	T = 40 °C	4.20	2.59
	T = 50 °C	5.06	7.67

Table 4
Comparison of Root Mean Square Error (RMSE) at different Values of Irradiation for Shell ST40 module at constant temperature T = 25 °C.

G (W/m^2)	G = 1000	G = 800	G = 600	G = 400	G = 200
Proposed approach	0.0669	0.0662	0.0256	0.0012	0.0232
Amine's method (Yahya-Khotbehsara and Shahhoseini, 2018)	0.0435	0.0359	0.0609	0.0724	0.0701
Ishaque's method (Ishaque et al., 2011)	0.0778	0.0446	0.0983	0.1202	0.0927
Babu's method (Babu and Gurjar, 2014)	0.1334	0.0411	0.1342	0.1911	0.1707
Wang's method (Wang et al., 2017)	0.0787	0.0344	0.0742	0.0985	0.1038

Table 5
Root Mean Square Error (RMSE) at different Values of Temperature for Shell ST40 module at constant irradiation G = 1000 W/m^2.

T (°C)	T = 20	T = 30	T = 40	T = 50	T = 60
Proposed approach	0.0751	0.0444	0.0598	0.1051	0.1548
Amine's method (Yahya-Khotbehsara and Shahhoseini, 2018)	0.0632	–	0.0723	–	0.0968
Ishaque's method (Ishaque et al., 2011)	0.0912	–	0.0893	–	0.0938
Babu's method (Babu and Gurjar, 2014)	0.1039	–	0.0878	–	0.0856
Wang's method (Wang et al., 2017)	0.0990	0.1089	0.1158	0.0928	0.1008

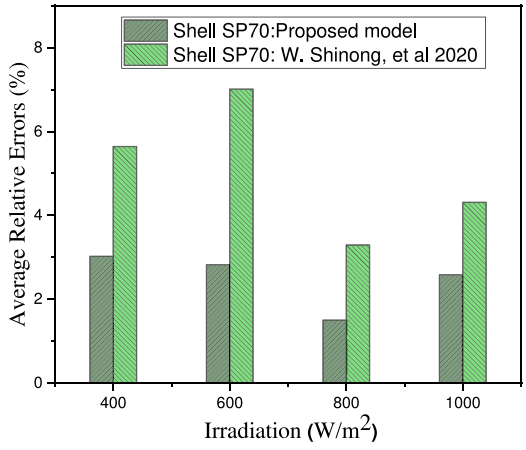

Fig. 14. Comparison of Absolute Relative Errors for Shell SP70 when Irradiation change and T = 25 °C.

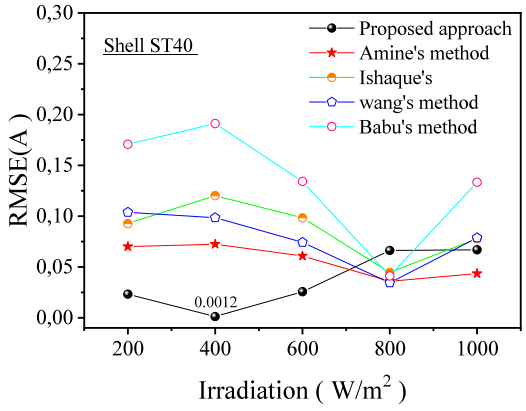

Fig. 15. Absolute Error of current at varying Temperature for Shell ST40.

than those obtained bay other methods and gives more important results. These small values of RMSE indicate that even in wide irradiation range, the proposed approach gives results that are very close to the experimental values provided by the manufacturers, which further proves the accuracy of the proposed method.

Tables 6 and 7 shows the comparison of the RMSE calculated using the proposed approach for Kyocera KC200GT and Shell SP70 modules when the temperature and irradiation change with the Gang Wang's methods (Wang et al., 2017). The results obtained indicate that the RMSE of the proposed method is less than those of the Wang's method. It proves that the proposed method is valid and effective for various operating conditions of PV modules.

The Figs. 16 and 17 shows the Absolute Error between the experimental and the calculated currents for each voltage point on I–V curve for Kyocera KC200GT module at several levels of irradiation (400, 600, 800 and 1000 W/m^2) while the temperature was set at 25 °C, and for Shell ST40 module at several levels of Temperature (20, 30, 40, 50 and 60 °C) while the irradiation was set at 1000 W/m^2. It can be seen from these figures that the maximum percentage Absolute Error of output current of the proposed method is 0.6502 A and its minimum value is 0.0083 A for KC200GT module. For Shell SP70 the IAE at lower temperature level is very law which is the minimum value is 8.2.10^{-5} A when the Temperature equal at 30 °C. These results provide good performance and exhibit superior accuracy of the thin film ST40 and for KC200GT.

Table 6
Root Mean Square Error (RMSE) at different Values of Temperature for Shell SP70 and KC200GT modules at constant temperature T = 25 °C.

G (W/m^2)	Kyocera KC200GT		Shell SP70	
	Proposed approach	Wang's method (Wang et al., 2017)	Proposed approach	Wang's method (Wang et al., 2017)
1000	0.0462	0.1331	0.0251	0.0658
800	0.0023	0.2296	0.0174	0.0598
600	0.0015	0.2800	0.0098	0.0610
400	0.0378	0.0073	0.0153	0.0473
200	0.0956	0.2460	0.0482	0.0312

Table 7
Root Mean Square Error (RMSE) at different Values of Temperature for Shell SP70 and KC200GT modules.

T (°C)	Kyocera KC200GT		Shell SP70	
	Proposed approach	Wang's method (Wang et al., 2017)	Proposed approach	Wang's method (Wang et al., 2017)
20	0.0523	–	0.0681	0.0754
30	0.0812	–	0.0347	0.0725
40	0.0675	–	0.0465	0.0791
50	0.0364	0.1503	0.0582	0.0723
60	0.0635	–	0.0675	0.0831

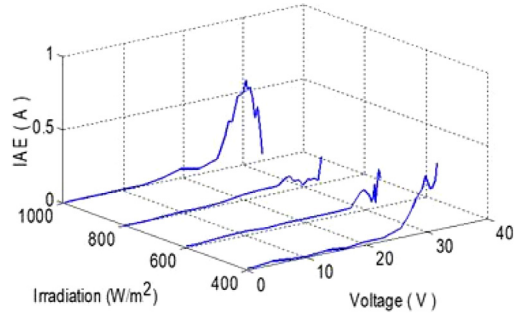

Fig. 16. Absolute Error of current at varying irradiance for KC200GT.

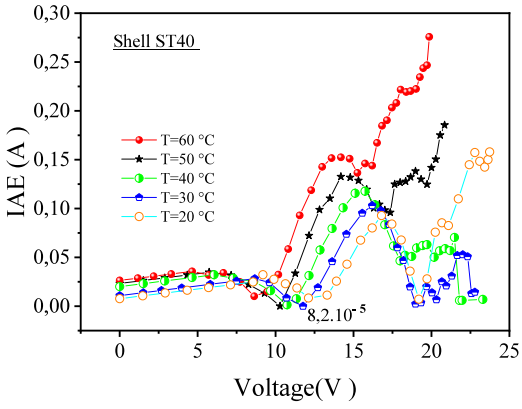

Fig. 17. Absolute Error of current at varying Temperature for Shell ST40.

5. Conclusion and future research

In this study the modeling and electrical characterization of different photovoltaic technologies is presented from measured I–V characteristics curves under real conditions using a mathematical approach based on the Lambert W-function for the extraction of parameters electrical for single diode model with five parameters. For the extraction of model parameters, this study starts with determination of the series and shunt resistances R_{sn} and R_{shn} at STCs using the slope between I_{scn} and MPP and between V_{oc} and MPP respectively. The parameters I_{pv} and I_o are calculated using equation adopted bay others authors (Moreira et al., 2017; Villalva et al., 2009a,b; Gao et al., 2018; Nassar-Eddine et al., 2016). The last parameter is ideality factor of the diode denoted n identified by using an iterative method. The highlight of this hybrid method adopted in this work is its simplicity and efficiency. It gives RMSE values lower than those obtained by other authors, which indicates that the calculated results are very close to the experimental values supplied by the manufacturers. Furthermore, for more accuracy, the average error relative is provided and it can be seen that the values obtained are better than other models. Validity of the result is obtained from three photovoltaic modules Shell ST40, Shell SP70 and Kyocera KC200GT.

Finally, the proposed method was validated using single diode and in the future work we can verified this approach with double and triple diode models. Also, an interesting application of this method, that is to construct realistic models of solar modules that can be used in simulation of Maximums Power Point Tracking (MPPT) algorithms.

CRediT authorship contribution statement

Dris Ben hmamou: Conceptualization, Validation, Writing – original draft, Writing – review & editing. **Mustapha Elyaqouti:** Conceptualization, Validation, Writing – original draft, Writing – review & editing. **Elhanafi Arjdal:** Conceptualization, Validation, Writing – original draft, Writing – review & editing. **Ahmed Ibrahim:** Conceptualization, Methodology, Writing – review & editing. **H.I. Abdul-Ghaffar:** Conceptualization, Methodology, Writing – review & editing. **Raef Aboelsaud:** Investigation, Review & editing. **Sergey Obukhov:** Investigation, Review & editing. **Ahmed A. Zaki Diab:** Software, Formal analysis, Funding acquisition.

Declaration of competing interest

The authors declare that they have no known competing financial interests or personal relationships that could have appeared to influence the work reported in this paper.

Acknowledgments

This research was supported by Tomsk polytechnic university development program. The Coauthor [Ahmed A. Zaki Diab] is funded by a full scholarship [mission 2020/2021] from the Ministry of Higher Education of Egypt). But, the current research work is not funded by the mentioned ministry of Egypt or any another organization/foundation.

References

Abbassi, Rabeh, Abbassi, Abdelkader, Jemli, Mohamed, Chebbi, Souad, 2018. Identification of unknown parameters of solar cell models: A comprehensive overview of available approaches. Renew. Sustain. Energy Rev. 90 (February), 453–474. http://dx.doi.org/10.1016/j.rser.2018.03.011.

Agwa, Ahmed M., El-Fergany, Attia A., Maksoud, Hady A., 2020. Electrical characterization of photovoltaic modules using farmland fertility optimizer. Energy Convers. Manage. 217 (April), 112990. http://dx.doi.org/10.1016/j.enconman.2020.112990.

Akdag, Ozan, Yeroglu, Celaleddin, 2021. Optimal directional overcurrent relay coordination using MRFO algorithm : A case study of adaptive protection of the distribution network of the Hatay Province of Turkey. Electr. Power Syst. Res. 192 (November 2020), 106998. http://dx.doi.org/10.1016/j.epsr.2020.106998.

Alhajri, M.F., Alrashidi, M.R., Sd, I.D.I., 2012. Optimal extraction of solar cell parameters using pattern search. Renew. Energy 44, 238–245. http://dx.doi.org/10.1016/j.renene.2012.01.082.

Askarzadeh, Alireza, Coelho, Santos, 2015. Determination of photovoltaic modules parameters at different operating conditions using a novel bird mating optimizer approach. Energy Convers. Manage. 89, 608–614. http://dx.doi.org/10.1016/j.enconman.2014.10.025.

Askarzadeh, A., Rezazadeh, A., 2012. Parameter identification for solar cell models using harmony search-based algorithms. Sol. Energy 86 (11), 3241–3249. http://dx.doi.org/10.1016/j.solener.2012.08.018.

Askarzadeh, Alireza, Rezazadeh, Alireza, 2013a. Artificial bee swarm optimization algorithm for parameters identification of solar cell models. Appl. Energy 102, 943–949. http://dx.doi.org/10.1016/j.apenergy.2012.09.052.

Askarzadeh, Alireza, Rezazadeh, Alireza, 2013b. Extraction of maximum power point in solar cells using bird mating optimizer-based parameters identification approach. Sol. Energy 90, 123–133. http://dx.doi.org/10.1016/j.solener.2013.01.010.

Babu, B. Chitti, Gurjar, Suresh, 2014. A novel simplified two-diode model of photovoltaic (PV) module. 4 (4), 1156–1161.

Balzani, Marianna, Reatti, Alberto, Marta, Via S., 0000. Neural network based model of a PV Array for the optimum performance of PV System.

Batzelis, Efstratios I., Student Member, Papathanassiou, Stavros A., Senior Member, 2015. A method for the analytical extraction of the single-diode PV Model parameters, pp. 1–9.

Bellia, Habbati, Youcef, Ramdani, Fatima, Moulay, 2014. A detailed modeling of photovoltaic module using MATLAB. NRIAG J. Astron. Geophys. 3 (1), 53–61. http://dx.doi.org/10.1016/j.nrjag.2014.04.001.

Benavides, Nicholas D., Chapman, Patrick L., Member, Senior, 2008. Modeling the effect of voltage ripple on the power output of photovoltaic modules. 55 (7), 2638–2643.

Bendib, T., Djeffal, F., Arar, D., Meguellati, M., 2016. Fuzzy-logic-based approach for organic solar cell parameters extraction. no. July 2013.

Ćalasan, Martin, Aleem, Shady H.E. Abdel, Zobaa, Ahmed F., 2020. On the root mean square error (RMSE) calculation for parameter estimation of photovoltaic models: A novel exact analytical solution based on Lambert W function. Energy Convers. Manage. 210 (January), 112716. http://dx.doi.org/10.1016/j.enconman.2020.112716.

Chegaar, M., Hamzaoui, A., Namoda, A., Petit, P., Aillerie, M., Herguth, A., 2013. Effect of illumination intensity on solar cells parameters. Energy Procedia 36, 722–729. http://dx.doi.org/10.1016/j.egypro.2013.07.084.

Chen, Yujie, Sun, Yize, Meng, Zhuo, 2018. An improved explicit double-diode model of solar cells: Fitness verification and parameter extraction. Energy Convers. Manage. 169 (February), 345–358. http://dx.doi.org/10.1016/j.enconman.2018.05.035.

Chennoufi, Khalid, Ferfra, Mohammed, Mokhlis, Mohcine, 2021. An accurate modelling of photovoltaic modules based on two-diode model. Renew. Energy 167, 294–305. http://dx.doi.org/10.1016/j.renene.2020.11.085.

Cubas, Javier, Pindado, Santiago, Victoria, Marta, 2014. On the analytical approach for modeling photovoltaic systems behavior. J. Power Sources 247, 467–474. http://dx.doi.org/10.1016/j.jpowsour.2013.09.008.

De Soto, W., Klein, S.A., Beckman, W.A., 2006. Improvement and validation of a model for photovoltaic array performance. Sol. Energy 80 (1), 78–88. http://dx.doi.org/10.1016/j.solener.2005.06.010.

Dongue, Sakaros Bogning, Njomo, Donatien, Ebengai, Lessly, 2013. An improved nonlinear five-point model for photovoltaic modules. 2013 (iii).

El-Naggar, K.M., AlRashidi, M.R., AlHajri, M.F., Al-Othman, A.K., 2012. Simulated annealing algorithm for photovoltaic parameters identification. Sol. Energy 86 (1), 266–274. http://dx.doi.org/10.1016/j.solener.2011.09.032.

Elhagry, et al., 1997. Fuzzy modeling of photovoltaic panel equivalent circuit.

Elsadd, Mahmoud A., Kawady, Tamer A., Maksoud, Abdel, Nagy, I. Taalab, 2021. Adaptive optimum coordination of overcurrent relays for deregulated distribution system considering parallel feeders. Electr. Eng. 103 (3), 1849–1867. http://dx.doi.org/10.1007/s00202-020-01187-0.

Gao, X., Cui, Y., Hu, J., Xu, G., Wang, Z., Qu, J., Wang, H., 2018. Parameter extraction of solar cell models using improved shuffled complex evolution algorithm. Energy Convers. Manage. 157, 460–479. http://dx.doi.org/10.1016/j.enconman.2017.12.033.

García-Sánchez, Francisco, Romero, Beatriz, Lugo-Muñoz, Denise, del, Pozo, Arredondo, Belén, Liou, Juin, Ortiz-Conde, Adelmo, 2017. Modelling solar cell S-shaped I-V characteristics with DC lumped-parameter equivalent circuits a review. Facta Univ. - Ser.: Electron. Energetics 30 (3), 327–350. http://dx.doi.org/10.2298/fuee1703327g.

Ghani, F., Rosengarten, G., Duke, M., Carson, J.K., 2014. The numerical calculation of single-diode solar-cell modelling parameters. Renew. Energy 72, 105–112. http://dx.doi.org/10.1016/j.renene.2014.06.035.

Hejri, Mohammad, Mokhtari, Hossein, Azizian, Mohammad Reza, Ghandhari, Mehrdad, Lennart, S., 2014. On the parameter extraction of a five-parameter double-diode model of photovoltaic cells and modules. 4 (3), 915–923.

Ishaque, Kashif, Salam, Zainal, 2011. An improved modeling method to determine the model parameters of photovoltaic (PV) modules using differential evolution (DE). Sol. Energy 85 (9), 2349–2359. http://dx.doi.org/10.1016/j.solener.2011.06.025.

Ishaque, Kashif, Salam, Zainal, Mekhilef, Saad, Shamsudin, Amir, 2012. Parameter extraction of solar photovoltaic modules using penalty-based differential evolution. Appl. Energy 99, 297–308. http://dx.doi.org/10.1016/j.apenergy.2012.05.017.

Ishaque, K., Salam, Z., Taheri, H., 2011. Simple, fast and accurate two-diode model for photovoltaic modules. Solar Energy Mater. Solar Cells 95 (2), 586–594. http://dx.doi.org/10.1016/j.solmat.2010.09.023.

Ismail, M.S., Moghavvemi, M., Mahlia, T.M.I., 2013. Characterization of PV panel and global optimization of its model parameters using genetic algorithm. Energy Convers. Manage. 73, 10–25. http://dx.doi.org/10.1016/j.enconman.2013.03.033.

Javier Toledo, F., Blanes, Jose M., Galiano, Vicente, 2018. Two-step linear least-squares method for photovoltaic single-diode model parameters extraction. IEEE Trans. Ind. Electron. 65 (8), 6301–6308. http://dx.doi.org/10.1109/TIE.2018.2793216.

Jervase, J.A., Bourdoucen, H., Al-Lawati, A., Askarzadeh, Alireza, Rezazadeh, Alireza, Macabebe, Erees Queen B., Sheppard, Charles J., et al., 2011. Identification of PV solar cells and modules parameters using the genetic algorithms: Application to maximum power extraction. Sol. Energy 85 (1), 266–274. http://dx.doi.org/10.1016/j.solener.2011.09.032.

Khan, Firoz, Singh, S.N., Husain, M., 2010. Determination of diode parameters of a silicon solar cell from variation of slopes of the I-V curve at open circuit and short circuit conditions with the intensity of illumination. Semicond. Sci. Technol. 25, http://dx.doi.org/10.1088/0268-1242/25/1/015002.

Kong, Yuan, Meliopoulos, A.P. Sakis, 2021. Study on effects of DSE-based instrumentation channel error correction on protective relays. Electr. Power Syst. Res. 192 (2020), 107002. http://dx.doi.org/10.1016/j.epsr.2020.107002.

Krakowski, M., Kurek, K., Nogal, Ł., 2021. Comparative analysis of the DAQ cards-based and the IEC 61850-based real time simulations in the Matlab/simulink environment for power system protections. Electr. Power Syst. Res. 192 (2020), 107000. http://dx.doi.org/10.1016/j.epsr.2020.107000.

Lo, Valerio, Orioli, Aldo, Ciulla, Giuseppina, 2012. On the experimental validation of an improved five-parameter model for silicon photovoltaic modules. Sol. Energy Mater. Sol. Cells 105, 27–39. http://dx.doi.org/10.1016/j.solmat.2012.05.028.

Louwen, Atse, Van Sark, Wilfried, 2019. Photovoltaic solar energy. In: Technological Learning in the Transition to a Low-Carbon Energy System: Conceptual Issues, Empirical Findings, and Use, in Energy Modeling. http://dx.doi.org/10.1016/B978-0-12-818762-3.00005-4.

Ma, Jieming, Man, Ka Lok, Ting, T.O., Zhang, Nan, Guan, Sheng-uei, Wong, Prudence W.H., 2013a. Approximate single-diode photovoltaic model for efficient I - V characteristics estimation.

Ma, Jieming, Ting, T.O., Man, Ka Lok, Zhang, Nan, Guan, Sheng Uei, Wong, Prudence W.H., 2013b. Parameter estimation of photovoltaic models via cuckoo search. J. Appl. Math. 2013, 10–12. http://dx.doi.org/10.1155/2013/362619.

Macabebe, E.Q.B., Sheppard, C.J., van Dyk, E.E., 2011. Parameter extraction from I-V characteristics of PV devices. Sol. Energy 85 (1), 12–18. http://dx.doi.org/10.1016/j.solener.2010.11.005.

Moreira, Hugo Soeiro, Oliveira, Tisciane Perpetuo E., Reis, Marcos Vinicios Gomes Dos, Guerreiro, Joel Filipe, Villalva, Marcelo Gradella, De Siqueira, Thais Gama, 2017. Modeling and simulation of photovoltaic systems under non-uniform conditions. In: 2017 IEEE 8th International Symposium on Power Electronics for Distributed Generation Systems, PEDG 2017. http://dx.doi.org/10.1109/PEDG.2017.7972524.

Nassar-Eddine, I., Obbadi, A., Errami, Y., Fajri, A. El, Agunaou, M., 2016. Parameter estimation of photovoltaic modules using iterative method and the Lambert W function: A comparative study. Energy Convers. Manage. 119, 37–48. http://dx.doi.org/10.1016/j.enconman.2016.04.030.

Peng, Wei, Zeng, Yun, Gong, Hao, Leng, Yong Qing, Yan, Yong Hong, Hu, Wei, 2013. Evolutionary algorithm and parameters extraction for dye-sensitised solar cells one-diode equivalent circuit model. Micro Nano Lett. 8 (2), 86–89. http://dx.doi.org/10.1049/mnl.2012.0806.

Peng, Lele, Zheng, Shubin, Chai, Xiaodong, Li, Liming, 2018. A novel tangent error maximum power point tracking algorithm for photovoltaic system under fast multi-changing solar irradiances. Appl. Energy 210 (2017), 303–316. http://dx.doi.org/10.1016/j.apenergy.2017.11.017.

Qin, Hengsi, Kimball, Jonathan W., 2011. Parameter determination of photovoltaic cells from field testing data using particle swarm optimization. http://dx.doi.org/10.1109/PECI.2011.5740496, no. March.

Rajasekar, N., Kumar, Neeraja Krishna, Venugopalan, Rini, 2013. ScienceDirect bacterial foraging algorithm based solar PV parameter estimation. Solar Energy 97, 255–265. http://dx.doi.org/10.1016/j.solener.2013.08.019.

Ruschel, Cristiano Saboia, Gasparin, Fabiano Perin, Costa, Eurides Ramos, Krenzinger, Arno, 2016. Assessment of PV modules shunt resistance dependence on solar irradiance. Sol. Energy 133, 35–43. http://dx.doi.org/10.1016/j.solener.2016.03.047.

Shinong, Wang, Qianlong, Mao, Jie, Xu, Yuan, Ge, Shilin, Liu, 2020. An improved mathematical model of photovoltaic cells based on datasheet information. Solar Energy 199 (February), 437–446. http://dx.doi.org/10.1016/j.solener.2020.02.046.

Stornelli, Vincenzo, Muttillo, Mirco, Rubeis, Tullio De, Nardi, Iole, 2019. A new simplified five-parameter estimation method for single-diode model of photovoltaic panels. pp. 1–20. http://dx.doi.org/10.3390/en12224271.

Tan, Yun Tiam, Member, Student, Kirschen, Daniel S., Member, Senior, Jenkins, Nicholas, Member, Senior, 2010. A model of PV generation suitable for stability analysis. 19 (4), 748–755.

Teixeira, Wagner, Simonetti, Domingos S.L., Dom, Av, Gaspar, Jose, 2010. Identification of photovoltaic model parameters by differential evolution. pp. 931–936.

Toledo, F.J., Blanes, José M., 2016. Analytical and quasi-explicit four arbitrary point method for extraction of solar cell single-diode model parameters. Renew. Energy 92, 346–356. http://dx.doi.org/10.1016/j.renene.2016.02.012.

Tong, Nhan Thanh, Pora, Wanchalerm, 2016. A parameter extraction technique exploiting intrinsic properties of solar cells. Appl. Energy 176, 104–115. http://dx.doi.org/10.1016/j.apenergy.2016.05.064.

Villalva, Marcelo Gradella, Gazoli, Jonas Rafael, Filho, Ernesto Ruppert, 2009a. Comprehensive approach to modeling and simulation of photovoltaic arrays. 24 (5): 1198–1208.

Villalva, Marcelo Gradella, Gazoli, Jonas Rafael, Filho, Ernesto Ruppert, 2009b. Modeling and circuit-based simulation of photovoltaic arrays. Eletr. Potência 14 (1), 35–45. http://dx.doi.org/10.18618/rep.2009.1.035045.

Wang, Gang, Zhao, Ke, Shi, Jiangtao, Chen, Wei, Zhang, Haiyang, Yang, Xinsheng, Zhao, Yong, 2017. An iterative approach for modeling photovoltaic modules without implicit equations. Appl. Energy 202, 189–198. http://dx.doi.org/10.1016/j.apenergy.2017.05.149.

Wei, Huang, Cong, Jiang, Lingyun, Xue, 2011. Extracting solar cell model parameters based on chaos particle swarm alogorithm. pp. 0–4.

Yahya-Khotbehsara, Amin, Shahhoseini, Ali, 2018. A fast modeling of the double-diode model for PV modules using combined analytical and numerical approach. Sol. Energy 162 (2017), 403–409. http://dx.doi.org/10.1016/j.solener.2018.01.047.

Ye, Meiying, Wang, Xiaodong, Xu, Yousheng, Ye, Meiying, Wang, Xiaodong, Xu, Yousheng, 2009. Parameter extraction of solar cells using particle swarm optimization parameter extraction of solar cells using particle swarm optimization. 094502: 0–8, http://dx.doi.org/10.1063/1.3122082.

Zagrouba, M., Sellami, A., Ksouri, M., 2010. Identification of PV solar cells and modules parameters using the genetic algorithms: Application to maximum power extraction. Sol. Energy 84 (5), 860–866. http://dx.doi.org/10.1016/j.solener.2010.02.012.